Industrial Visual Defect Inspection of Electronic Components with Siamese Neural Network

Warley Barbosa[a], Lucas Amaral, Tiago Vieira[b], Bruno Georgevich and Gustavo Melo

Edge Innovation Lab, Federal University of Alagoas, Av. Lourival Melo Mota, Maceió, Brazil

Keywords: Printed Circuit Board, Electronic Component Defect, Visual Inspection System, Siamese Neural Network.

Abstract: We present a system focused on the Visual Inspection of Pin Through Hole (PTH) electronic components. The project was developed in a partnership with a multinational Printed Circuit Board Printed Circuit Board (PCB) manufacturing company which requested a solution capable of operating adequately on unseen components, not included in the initial image database used for model training. Traditionally, visual inspection was mostly performed with pre-determined feature engineering which is inadequate for a flexible solution. Hence, we used a one-shot-learning approach based on Siamese Neural Network model trained on anchor-negative-positive triplets. Using a specifically designed web crawler we collected a new and comprehensive database composed of electronic components which is used in extensive experiments for hyperparameters tuning on training and validations stages, achieving satisfactory performance. A web application is also presented, which is responsible for the management of operators, recipes, part number, etc. A hardware responsible for attaching the PCBs and a 4K camera is also developed and deployed on industrial environment. The overall system is deployed in a PCB manufacturing plant and its functionality is demonstrated in a relevant scenario, reaching a level 6 in Technology Readiness Level (TRL).

1 INTRODUCTION

Detecting defects is very important in industrial manufacturing. Even though many inspections are performed manually, Machine Vision (MV) technologies can be applied to determine whether or not manufactured elements satisfy conformity requirements enforced by government's policy makers or the company itself. High customer demand, high production rate and an ever-growing and fierce competition are motivating factors for the development of high-confidence, low-error MV systems.

This is particularly true for PCB manufacturing industries. It is currently experiencing an increase in demand but due to recent international health and political events, a shortage in production. Indeed, even though there were signs of lack of chip production prior to the world pandemic, the industry utilization hasn't fallen bellow to 90% since the summer of 2020, reflecting a growing appetite for connected home appliances and increasingly sophisticated automated driving features and digital connectivity in cars (Harris, 2022).

[a] https://orcid.org/0000-0001-5567-6065

[b] https://orcid.org/0000-0002-5202-2477

With the advancement of microelectronics, the size of electronic components is being reduced over the years, which increases the challenge of traditional image processing and computer vision approaches focused on operating on well-defined/low-variance systems. Because of this, supervised learning algorithms have being used to meet the demands for higher accuracy. When supervised learning algorithms are used to solve any kind of problem, they must be trained on well-annotated Databases (DBs) once the quality of the database will define the quality of the trained model. Thus, other challenge is the lack of available DBs containing images of electronic components specifically of type PTH. Unfortunately, the ones that do have a non-permissive license for commercial uses (Pramerdorfer and Kampel, 2015). Also, the majority of datasets are built to solve specific problems (such as Surface Mounted Device (SMD) or verifying discontinuities on conduction tracks) and they cannot be combined nor repurposed for different scenarios. In our context, we developed a web crawler to collect images of electronic components from the Internet, to increase the number of examples and improve the model's generalization capacity by avoiding overfitting.

Barbosa, W., Amaral, L., Vieira, T., Georgevich, B. and Melo, G.
Industrial Visual Defect Inspection of Electronic Components with Siamese Neural Network.
DOI: 10.5220/0011696400003417
In *Proceedings of the 18th International Joint Conference on Computer Vision, Imaging and Computer Graphics Theory and Applications (VISIGRAPP 2023) - Volume 4: VISAPP*, pages 889-896
ISBN: 978-989-758-634-7; ISSN: 2184-4321

In addition, unlike using pre-built features based on textures, colors, etc., Neural Networks (NNs) are able to learn how to predict classes of objects or attributes. When a given model must be applied to more classes, the NN must be re-trained on a bigger database with such novel data. To tackle this limitation and avoid the collection of new data, we use a Siamese Neural Network (SNN) (BROMLEY et al., 1993) which, during inference, takes two inputs, a sample and a reference. Both images run through a convolutional backbone which provides a vector representation for each image. Then, both representation vectors are compared with a similarity function that will determine how similar the sample image is to the reference one. SNNs can learn the most relevant visual features to properly quantify the similarity between the inputs if adequately trained. We cite some related works in the following.

Researchers have separated visual inspection into two stages; detection and fine-grained matching (verification). For instance, Reza *et al.* focused on applying hard loss to detect components and identifying subtle changes such as slightly different logos printed onto Integrated Circuits (ICs) housing (Reza et al., 2020). The goal was to identify counterfeit components and prevent PCB malfunction, security vulnerabilities, among others. They used loss boosting to alleviate the problem of undetected small components when using traditional Convolutional Neural Networks (CNN)-based detectors. Since they consider each PCB a sample, they split all objects (electronic components) into “easy” and “hard”, according to their associated difficulty to locate. Researchers annotated 483 PCB images resulting in approximate 5000 labeled IC samples – we could not access the dataset because of a broken link. After evaluating different backbones and hyperparameters settings, they achieved up to 92.31% verification accuracy on a held-out test set.

Luan *et al.* (Luan et al., 2021) used SNNs (BROMLEY et al., 1993) for defect detection. They mention a proprietary database containing approximately 400 samples for each of five classes; normal and four synthetic and specific defect types. Performances of different loss functions are presented to assess the impact on unbalanced datasets with much fewer defect samples. No mention is given as to the cross-validation scheme used and different performances seem to be more influenced by two different classification methods (CNN with two neurons as final classifiers *versus* Support Vector Machine (SVM)-based classifier) than by different choices of loss functions.

Nagy (Nagy and Czúni, 2021), *et al.*, used SNN as a strategic option for the identification of anomalies on a wide variety of object types on databases containing images of traffic signs an metal disk-shape castings with and without defects. Unfortunately, our dataset does not have samples with actual defects.

Kalber *et al.* (Kälber et al., 2021) used U-Net for segmentation of electronic components on PCB images published by Tang *et al.* (Tang et al., 2019). Our approach is different since we do not perform localization of components which are manually annotated by the operator when the recipe is constructed. Besides that, our focus in this work is to verify components that were not present in the dataset.

Saeedi and Giusti proposed an anomaly detection system for industrial vision inspection (Saeedi and Giusti, 2022). To alleviate problems associated with deffect loss due to downsizing, they propose the use of patches as input to an Autoencoder (AE).

Our contributions are summarized in the following:

1. We collect a comprehensive database composed of images of PTH electronic components in a cooperation with a PCB manufacturing company and by developing a web crawler which collects more data from the Internet. We manually annotate them to select components of interest. A specific data augmentation approach is also presented.
2. A visual inspection model using SNN that provides flexibility to different types of electronic components validated using a comprehensive set of validation experiments and hyperparameters tuning.
3. A hardware to stabilize the PCB and control environment illumination and a flexible, customizable web app are developed and presented.

2 METHODOLOGY

We define five methodological steps to guide our approach: 1. Dataset acquisiton and cleaning. 2. Image annotation. 3. Application development. 4. Database Augmentation. 5. SNN training and validation.

The first step consists in acquiring images from the Internet using a web crawler, developed by us. Once the images were already downloaded and the dataset is well organized, we started the second step, which consists in annotating the image database that we collected using the YOLO format, which is simple to read and parse from the computer perspective. We annotate the images using an object detection strategy

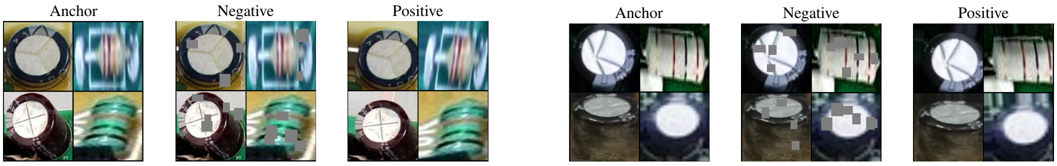

(a) Training dataset sample triplets. (b) Validation dataset sample triplets.

Figure 1: Sample triplets comprised in the PTH image dataset for (a) training and (b) validation. For each case, left, middle and right columns correspond to anchor, negative (added noise) and positive images. Notice the small gray patches present on negative samples (middle columns). Each image actual size is 128×128.

because we will need to crop the components afterwards to build our dataset since each image (of a single PCB) has several electronic components and our work aims at classifying whether the component is correct or not. Hence, the third step was to develop an application capable of cropping the PCB components from the image so each component is used individually to train the model. The fourth and fifth steps were to augment the dataset and train a Siamese neural network (SNN), respectively.

After annotating the images, we had a comprehensive database composed of electronic PTH components of PCB. Although we have a good amount of images, we still need images with actual defects (non-conform components), since our model must be able to identify whether they are defective or not. Because we did not find those images, we developed some image processing routines that randomly insert noise in the images, to make them different from the correct ones, enforcing the model to understand which are generic visual features to search for. The augmentation routine developed generates triplets, which are composed by the anchor (I_A), one positive example (I_P) and a negative example (I_N). The anchor is a referent component, the positive example is an image similar to the anchor (of the same component) and the negative one is a different component, the same component with defect or with added noise. The development of the augmentation routine was done in a similar way to the work of (Schroff et al., 2015).

2.1 Database

The database construction started with the development of the web crawler, that would collect additional images from the internet. Once the web crawler does not have any kind of smart component in its operation, some parts of the collected images can be discarded. Hence, we performed some cleaning rounds over all images before the annotation process. We annotated the images using the YOLO format, since we consider it easier to parse and store. We considered the electronic components shown in Table 1.

Table 1: List of electronic components in the dataset.

ID	Label
1	Capacitor
2	Ceramic Capacitor
3	Converter
4	Diode
5	Heat sink
6	Crystal Oscillator
7	Relay
8	Resistor
9	SMD capacitor
10	SMD diode
11	SMD transistor
12	Transistor

In addition of the classes of components, we also defined which error categories the model should be able to identify. The error classes are listed in the Table 2. These errors were generated using the data augmentation routines that we developed, once it is reasonably difficulty to find defective samples in the internet.

To construct the triplets, first we determine the anchor by selecting a component belonging to a given class from our list (*cf.*, Fig. 1). After that, we determine the positive image, by slightly rotating or translating the anchor to make the model understand that it is a different image of the same anchor component. Using positive image is important because the network must aim at reducing the distance between two embeddings belonging to the same category too. Regarding the negative sample, disruptive rotations or translations turn an anchor to negative because the recipe does not admit it (e.g., a component could be wrongly welded). We propose three different strategies for constructing a negative sample:

Table 2: List of errors in the dataset construction.

ID	Label
1	missing component
2	wrong component
3	shifted or rotated component
4	component lifted
5	component misplacement

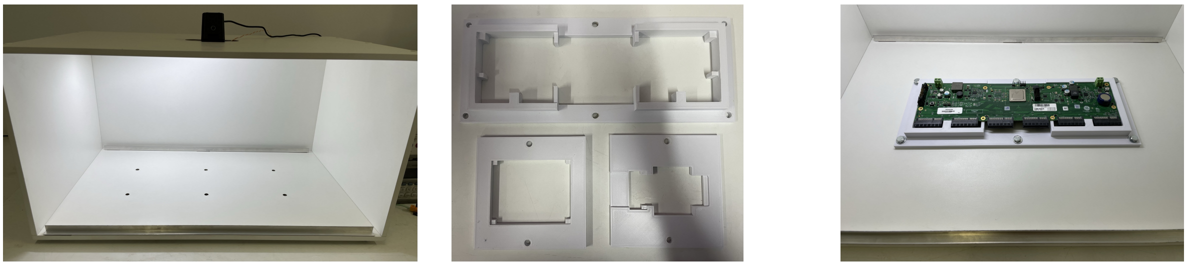

(a) PCB inspection cabinet. (b) Three cradles. (c) Cabinet with a cradle installed.

Figure 2: Elements constituting the hardware developed for this project. (a) Cabinet with 4k camera. (b) Examples of 3D printed cradles. (c) PCB installed into a cradle.

1. Select an image from a class different from the anchor.
2. Use a modified version of the same anchor image, like the addition of random gray patches.
3. Use a hybrid scheme where both strategies 1 and 2 are combined.

The augmentation routines were planned to allow the model to discern between correct and incorrect or defective components, but also to make the model more robust to naturally occurring small translations and rotations for non-defective components. At the end, we were able to generate approximately 4,000 triplets.

2.2 Hardware

A custom cabinet was designed and built to enable PCB photos to be taken in a controlled environment, avoiding outside interference and thus ensuring the correct operation of the model. This kind of cabinet is designed to be used in real industry environments, which allows us to test our model in an ambient that mimics a real scenario.

The cabinet (Figure 2a) is a box built with MDF (Medium-Density Fiber-board), with an open front. The box has six holes with nuts at the bottom, allowing cradles for the PCBs to be screwed onto the bottom. This approach allows the cradle to remain fixed during PCB verification and makes it possible to change for other cradles associated with different PCB clients.

The cradle is custom-made and can be printed using a 3D printer, allowing the user to design an specific cradle for each PCB design. This strategy allows us to place different PCBs of the same type in the same position on the cabinet. We used the GT-MAX3D CORE GT4 printer and white ABS filament to print the cradles used during the experiments (Figure 2b).

At the top of the cabinet there is an opening where a Logitech BRIO 4K resolution camera where placed. An LED strip was installed on the ceiling to provide a more homogeneous light. It is possible to see in the Figure 2c the cabinet with a cradle installed during a PCB inspection.

2.3 Web Application

After model training (*cf*, Section 2.4), it is inserted into a web application that can perform the inspection of the PCBs and manage all the metadata related to it. The system manages recipes which contains information related to the confidence threshold of each component. Additionally, there is also the management of components, which defines the positive examples for each component class. This application illustrates how it is possible to tackle industrial problems by combining modern NN models with traditional application development.

2.4 SNN

Regarding the model, we choose a SNN classifier, because it is a metric-based model which allows the addition or removal of classes without being necessary to retrain the model. We performed the training

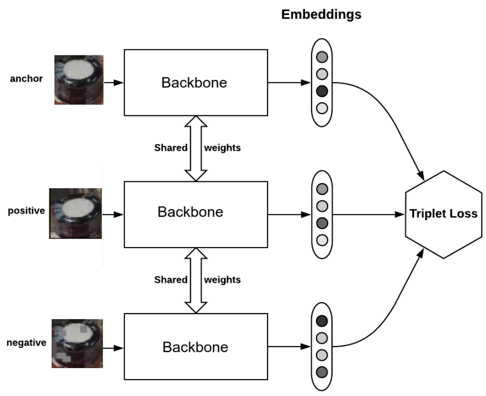

Figure 3: Our model architecture.

and validation several times using the grid-search algorithm to find the best set of hyperparameters. The training process was executed by successively inserting positive and negative examples as inputs into the model.

Since the SNN is a metric-based model, it has the capacity of comparing two inputs and evaluate if they are similar or not. So, if we provide two images as input to the model, it will process both entries and compare them by using a comparison function that is defined in its architecture. The SNN training process is done by using triplet loss, which is defined in the Eq. (1).

$$\mathcal{L}(I_A, I_P, I_N) = max(\|f(I_A) - f(I_N)\|^2 - \|f(I_A) - f(I_N)\|^2 + \alpha, 0) \quad (1)$$

Where: f is the network embedding; I_A, I_P and I_N are the entries (images), and; α is the margin. By optimizing parameters to reduce the triplet margin loss, the training procedure tries to decrease the distance between positive and anchor and increase the distance between negative and anchor. This approach was inspired in the FaceNet (Schroff et al., 2015), since they try to solve a similar problem. The model architecture can be seen in the Figure 3.

The architecture consists basically of a *backbone*, with parameters shared by all the model entries. The backbone processes the input and summarizes the most relevant information which are then flattened into the feature vectors and are compared by the loss function. We tested four different backbone topologies, as an attempt of understand which one is most suitable to extract relevant features from the inputs. Those were; InceptionResnet V2; MobileNet V3 Large; MobileNet V3 Small and ResNet50.

2.5 Evaluation Metrics

The output of the trained SNN was defined in two categories: nonconformity (N) and conformity (P). The nonconformity category determines that at least one of the PCB components is defective or missing. The conformity category means that all components are where they were expected to be in the PCB, determining that such PCB was assembled correctly. Besides that, the classification results were assessed by analyzing the Precision×Recall curve, computed by the equations 2 and 3, below.

$$Prec = \frac{TP}{TP + FP} \quad (2)$$

and

$$Rec = \frac{TP}{TP + FN}, \quad (3)$$

where, TP denotes True Positive, FP False Positive, and FN False Negative. The Precision×Recall (PR) curve was computed using different thresholds of the similarity score δ between a pair of images. We also use the Receiver Operating Characteristic Curve (ROC) and Area Under the Curve (AUC) to evaluate model performance.

2.6 Experiments

We divided the experiments into two stages aiming at reducing the number of hyperparameters and, consequently, the number of experiments necessary to search for the best performance. In the first stage, the selected hyperparameters were: 1. `Enable/Disable batch normalization`; 2. `Enable/Disable embeddings normalization`, and; 3. `Which layers must be trained in the backbone`. Our reason to select these three was because they were closely related: the backbone used dictates how many layers we can fine-tune, for example. The hyperparameters used in the first phase can be seen in the Table 3.

We began the experiments with two most frequent categories: Resistor and Capacitor. After that, we performed more experiments where we added the next class with the highest number of samples to each new experiment, while using those hyperparameters values from the best results in the first stage.

To enable better experiments, we used the `Lightning` (Falcon and The PyTorch Lightning team, 2019) framework to implement and train the model and `timm` (Wightman, 2019) to load the pretrained MobileNet v3 model. The `Lightning` framework allows us to easily train and test the model, as well as to

Table 3: Hyperparameters used in the first phase of the experiments. Others were implemented (e.g., TTA), but not used.

Hyperparameter	**Value**
Augmentation strategy	coarse-dropout-v1
Backbone	MobileNet v3 (large, 100)
Batch normalization	{True, False}
Batch size	64
Embedding dimension	512
Embeddings normalization	{True, False}
Image size	128×128
Learning rate	0.01
Loss function	Triplet Margin Loss
Number of epochs	100
Optimizer	Adam
Trainable layers	{0, 1, 10, 27, 43, 67, 91, 103, 107, 108, 109}
Triplet distance	Euclidean
Triplet margin	0.2
Triplet strategy	same

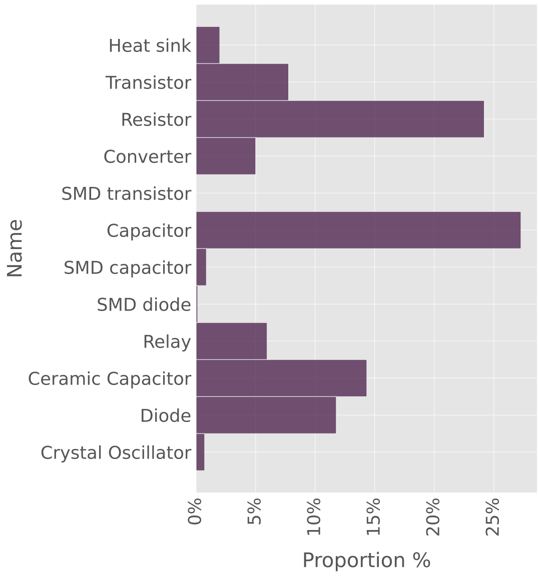

Figure 4: The dataset sample distribution histogram.

use many variations of datasets if needed. The `timm` library is a collection of PyTorch modules for computer vision, which allows us to load any pretrained model and use it in our experiments. For experiment tracking we used `guildai` package (Smith, 2018), which also enable us to perform hyperparameters tuning and compare experiments.

Since our dataset images vary in shapes, we needed to resize them before passing as input to the model. We determined the default shape as $128\times128\times3$ because almost 90% of the dataset has width and height below 128. A batch size of 64 samples (triplets) allows us to introduce class variety without inserting too much noise. We implemented and used the *TripletMarginLoss* with default euclidean distance, but with a customized margin as hyperparameter (Musgrave et al., 2020). At the end, we also implemented the Test-Time Augmentation as an option to the validation stage aiming at decreasing validation metrics variance, because our negative samples are artificially created with image processing augmentation routine.

3 RESULTS AND DISCUSSION

3.1 Database Statistics

Each experiment was tracked and monitored via `guildai` and `TensorBoard` (Abadi et al., 2016), which allow us to compare the experiment's metrics by visualizing the training and validation losses, as well as image similarity metrics. Figure 5 shows the training and validation losses of the baseline model, which was trained using the MobileNet v3 (large, 100) backbone. In addition, we stored the confusion matrix, distance, and similarity histogram between pairs in the triplet, PR and ROC curves, and model weights to evaluate any major changes in the updates.

The database has 18,303 samples (images of electronic components of PCB) extracted from internet sources. These images were collected from the Internet using a web crawler developed for this purpose. The database was divided into 12 classes, as specified in Table 1. The database distribution among the classes can be seen in Figure 4. To better observe the improvement of the model, we determined the validation set at the beginning of the model development.

3.2 Experiments

Results from the best experiments in phase one (baseline) are shown in Table 4. We validated the model based on its accuracy, precision, and recall. Some instabilities are present in the validation, with accuracy varying from 0.65 to 0.96. We also stored the area under the Receiver Operating Characteristic (ROC) curve during validation to inspect the model's ability to detect conformities for a given probability of false positive (see Figure 5a). Similarly, we also plot a Precision$\times$Recall (PR) curve to analyze their tradeoff, as shown in Figure 5b.

We also evaluated the results using a confusion matrix, as shown in Figure 5c. The confusion matrix shows us that our model correctly predicted 981 (36.50%) negative pairs and, 1321 (49.14%) positive pairs. However, there were 23 (0.86%) false negatives and 363 (13.50%) false positives. These results are detailed in Figure 6, which shows the similarities between the positive and negative pairs.

In Table 4 we summarize phase 1 by showing only the best models which achieved an accuracy above 70%, which is a subset of 7 experiments from a total of 44 that we performed. Except for the experiments `1`, `3`, and `6`, the remaining trials show errors and metrics curves similar to the best experiment from phase 1.

Finally, in Table 5 we show the results for phase 2, where we add one more class to each experiment. We also rerun the experiment which gave us the best result from phase 1 with purposes of comparison. The instability showed in the training and validation stages of the experiments of phase 1 is also present in the experiments of phase 2. As shown in Figure 1, our augmentation in the negative sample (middle column) was intended to mimic defective components, while the positive sample received a small augmentation.

Table 4: Metrics for the top models.

experiment	amount_layer_trainable	batch_norm	normalize	train/accuracy	train/precision	train/recall	val/accuracy	val/precision	val/recall
1	67	no	no	0.9995	0.9991	1.0	0.9561	0.9268	0.9918
2	91	yes	yes	0.9281	0.8810	0.9995	0.8563	0.7858	0.9828
3	91	yes	no	0.9894	0.9863	0.9928	0.7511	0.6708	0.9903
4	103	yes	yes	0.9967	0.9939	0.9997	0.7395	0.6586	1.0
5	109	yes	yes	0.9990	0.9981	1.0	0.7358	0.6563	0.9955
6	108	no	no	1.0	1.0	1.0	0.7072	0.6314	1.0
7	108	yes	yes	0.9995	0.9993	0.9997	0.7034	0.6289	1.0

What is worse, the results from the best experiment in phase 1 (experiment 1 in Table 4) could not be reproduced in a new run (2 in Table 5). These results seem to indicate that the augmentation may not be good enough, since the model does not converge as we expect.

4 CONCLUSION

We presented results of a visual inspection system focused on electronic components for the purpose of PCB production quality control. The project was developed in a partnership with a multinational PCB manufacturing company which possesses a wide variety of international clients.

We developed a complete system — a web app, a machine learning model, and a hardware plataform — which enabled the company to inspect defects in unseen components. This is a major advantage over current rigid inspection process. An SNN architecture, which is a flexible and scalable solution is adequate to tackle the problem, was trained using with data gathered from the company and from a web crawler, customized for the purpose of collecting images of electronic components from the internet. The model was evaluated using a set of experiments showing promising results.

The overall system is currently deployed in the company's manufacturing plant. Its feasibility and adequacy of the method was demonstrated on a relevant scenario, which can categorize the solution within a level 6 of Technology Readiness Level (TRL). Further experiments are being conducted in a more challenging scenario (production — aimed at TRL 7) and newer results will be eventually reported.

One of the main obstacles in the development of the system was the lack of images of non-conform components. To overcome this problem, we developed an simple augmentation strategy to simulate defects that could be seen in production by modifying random regions of the image and adding gray patches. More work is needed in this vein, that is, how could we best simulate defects that would generalize well for all types of components? Each component has its own rules for what can be categorized as an defect. For example, a capacitor can't be rotated by 180 degrees, but a resistor can.

Another fruitful approach is to use other distances and losses for the SNN model. The current model uses a triplet loss function with a default euclidean distance, which is a common strategy in the metric learning literature. Also, a common loss in the face recognition literature, the ArcFace loss (Deng et al., 2019), could be used.

At the end, we think that by curating better data, developing a new augmentation strategies, and taking advantage of the training scripts we implemented, our work can be used in the industry to improve the quality control process of PCB production.

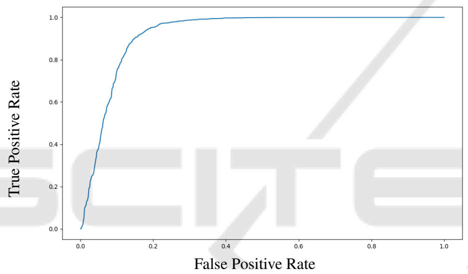

(a) ROC curve.

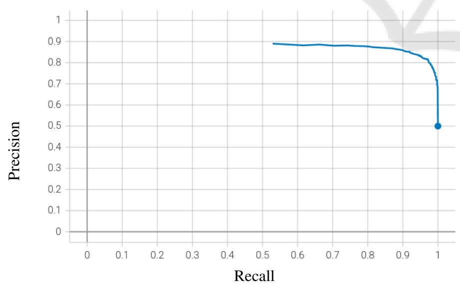

(b) Precision×Recall (PR).

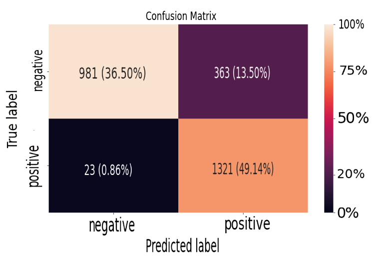

(c) Confusion matrix.

Figure 5: Baseline results.

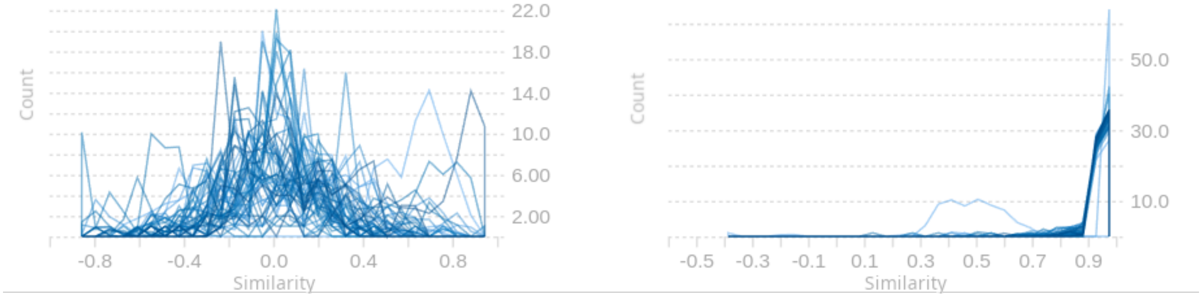

Figure 6: Histograms of cosine similarities for negative (left) and positive (right) pairs.

Table 5: Metrics for the top models in phase 2.

experiment	classes	train/accuracy	train/precision	train/recall	val/accuracy	val/precision	val/recall
1	Resistor, Capacitor, Capacitor Cerâmico	0.9855	0.9727	1.0	0.7199	0.6423	1.0
2	Resistor, Capacitor	0.9968	0.9942	0.9996	0.6860	0.6170	0.9903
3	Resistor, Capacitor, Capacitor Cerâmico, Diodo	0.9991	0.9989	0.9993	0.5554	0.5295	1.0

ACKNOWLEDGEMENTS

This work was partially funded by SOFTEX[1].

REFERENCES

Abadi, M., Agarwal, A., Barham, P., Brevdo, E., Chen, Z., Citro, C., Corrado, G. S., Davis, A., Dean, J., Devin, M., et al. (2016). Tensorflow: Large-scale machine learning on heterogeneous distributed systems. *arXiv preprint arXiv:1603.04467*.

BROMLEY, J., BENTZ, J. W., BOTTOU, L., GUYON, I., LECUN, Y., MOORE, C., SÄCKINGER, E., and SHAH, R. (1993). Signature verification using a “siamese” time delay neural network. *International Journal of Pattern Recognition and Artificial Intelligence*, 07:669–688.

Deng, J., Guo, J., Xue, N., and Zafeiriou, S. (2019). Arcface: Additive angular margin loss for deep face recognition. In *Proceedings of the IEEE/CVF conference on computer vision and pattern recognition*, pages 4690–4699.

Falcon, W. and The PyTorch Lightning team (2019). PyTorch Lightning.

Harris, M. (2022). These 5 charts help demystify the global chip shortage.

Kälber, F., Köpüklü, O., Lehment, N., and Rigoll, G. (2021). U-net based zero-hour defect inspection of electronic components and semiconductors. pages 593–601. SCITEPRESS - Science and Technology Publications.

Luan, C., Jing, Z., and Zuo, J. (2021). A defect-sensitive loss function based on siamese network to defect detection with imbalanced samples. *Journal of Physics: Conference Series*, 1802(4):042085.

Musgrave, K., Belongie, S., and Lim, S.-N. (2020). Pytorch metric learning.

Nagy, A. and Czúni, L. (2021). Detecting object defects with fusioning convolutional siamese neural networks. pages 157–163. SCITEPRESS - Science and Technology Publications.

Pramerdorfer, C. and Kampel, M. (2015). A dataset for computer-vision-based pcb analysis. In *2015 14th IAPR International Conference on Machine Vision Applications (MVA)*, pages 378–381. IEEE.

Reza, M. A., Chen, Z., and Crandall, D. J. (2020). Deep neural network–based detection and verification of microelectronic images. *Journal of Hardware and Systems Security*, 4:44–54.

Saeedi, J. and Giusti, A. (2022). Anomaly detection for industrial inspection using convolutional autoencoder and deep feature-based one-class classification. pages 85–96. SCITEPRESS - Science and Technology Publications.

Schroff, F., Kalenichenko, D., and Philbin, J. (2015). Facenet: A unified embedding for face recognition and clustering. In *Proceedings of the IEEE conference on computer vision and pattern recognition*, pages 815–823.

Smith, G. (2018). Guild ai - experiment tracking, ml developer tools. https://github.com/guildai/guildai.

Tang, S., He, F., Huang, X., and Yang, J. (2019). Online pcb defect detector on a new pcb defect dataset.

Wightman, R. (2019). Pytorch image models. https://github.com/rwightman/pytorch-image-models.

[1]https://softex.br/